Application of a thermal spike model to experimental ion-induced grain growth data

Dale E. Alexander
Materials Science Division, MSD-212, Argonne National Laboratory, Argonne, IL 60439 (USA)
Gary S. Was
Department of Nuclear Engineering, University of Michigan, Ann Arbor, MI 48109 (USA)

Abstract

A model of ion-induced grain growth is developed incorporating the irradiation effect concept of thermal spikes. The results of the model predict that for normal grain growth the ion-induced mobility is linearly proportional to the quantity $F_D^2/\Delta H_{coh}^3$, where F_D is the ion and recoil energy deposited in nuclear interactions and ΔH_{coh} is the cohesive energy. This linearity is shown to be supported by the data from six of seven previous ion-induced grain growth experiments. The model analysis is combined with the experimental data to determine values of the proportionality constant, β_{IIGG}, relating the cohesive energy to the activation energy for grain growth ($Q = -\beta_{IIGG}\Delta H_{coh}$). The values are found to span a range, $0.05 \leqslant \beta_{IIGG} \leqslant 0.10$, which is less than the value previously determined for the thermal spike treatment of ion beam mixing ($\beta_{IM} = 0.14$), and therefore consistent with the idea that atom migration across grain boundaries is easier than migration within the lattice. The consistency of results from the analysis of an entirely different phenomenon adds further credence to the thermal spike treatment of ion-induced grain growth. Finally, it is recommended that additional experiments be performed to evaluate further the model's validity.

1. Introduction

Ion irradiation has been observed to induce grain growth in thin polycrystalline metal, semiconductor and multilayer films [1–8]. The ability to control grain size in thin films using irradiation without heating has significant practical implications. For example, in microelectronics, grain size is an important factor which determines the electromigrative characteristics of thin film devices. The ability to increase the grain size using ion irradiation can avoid detrimental effects associated with interdiffusion and second-phase formation that may accompany thermal processing. In addition to such practical implications, the study of ion-induced grain growth should provide further insight into the fundamental nature of ion–solid interactions. Despite a number of systematic irradiation studies [1–8] performed on thin films, a complete understanding of ion-induced grain growth is still lacking.

Previous studies in large part have attempted to relate the damage effects which occur during ion irradiation with the observations of grain growth. Defect production during an ion-induced displacement cascade occurs in two phases [9]. Initially, during the collisional phase of the cascade, atomic displacements occur via a series of high energy binary collisions. In the later stages of the cascade, the kinetic energy of the remaining recoiling atoms is thermalized within the crystalline lattice. This latter phase is termed the thermal spike phase and further short-range atomic motion may be induced by thermal agitation within the local volume of the spike. Unlike the high energy collisional phase, the average kinetic energy during the thermal spike phase is low (less than or equal to 1 eV) and hence atomic migration is strongly affected by material-related thermochemical quantities which are of the same magnitude. One of the important questions that emerges in understanding ion-induced grain growth, is the relative importance of the collisional and thermal spike phases to the grain boundary migration phenomena.

Atwater *et al.* [7] previously suggested that the ion-induced grain growth process is collisional in nature and proposed a transition-state model in which defects produced on or near grain boundaries contribute to grain boundary migration. While Atwater's model is successful in describing observations in irradiated silicon, germanium and gold films, more recent experiments suggest that displacement phenomena alone are inadequate for describing ion-induced grain growth. For example, Li *et al.* [2] observed large differences in grain growth among irradiated platinum and gold films, despite the fact that their similar masses and displacement energies suggested that they should behave collisionally the same. Liu [8] and Alexander *et al.* [1] observed variations in grain growth rates that scaled with the cohesive energy ΔH_{coh} of the targets, indicating

0257-8972/92/$5.00

that material parameters in addition to collisional-related material properties are also important. These observations, analogous to results in ion beam mixing experiments [10], led Liu and coworkers to suggest that ion-induced grain growth, like ion mixing, may be described as a thermal spike phenomenon.

The thermal spike approach offers considerable potential for describing the ion-induced grain growth phenomenon. In this paper, we present the results of a thermal spike model we previously developed to describe grain growth behavior in homogeneous and multilayered films [11, 12]. The model is then applied to experimental results from a variety of previous studies in order to evaluate its validity.

2. Thermal spike model of ion-induced grain growth

During normal grain growth, boundary migration is assumed to occur by thermally activated atom jumps across a boundary. The velocity dL/dt of the grain boundary in one dimension is described by,

$$\frac{dL}{dt} = -M\frac{\partial \mu}{\partial x} \tag{1}$$

where M is defined as the grain boundary mobility, and the gradient in the chemical potential $\partial\mu/\partial x$ is the driving force associated with the boundary motion.

The thermal spike approach proposes that the heated cylindrical spikes produced during irradiation induce the atom jumps across grain boundaries. In order to apply thermal spike concepts, it is necessary to derive a parameter η defined as the number of atom jumps induced per unit length of spike per spike. With this parameter the macroscopic grain growth is related to the microscopic effects of irradiation according to

$$\frac{dL}{dt} = \frac{\eta\delta\Phi}{\rho} \tag{2}$$

where δ is the grain boundary width, Φ is the ion dose rate and ρ is the atomic density.

The parameter η is derived following the analytical treatment of Vineyard [13] and is detailed elsewhere [11, 12]. In brief, a cylindrical thermal spike is produced by a recoiling atom depositing an energy F_D per unit path length in nuclear interactions. The spike induces an Arrhenius-type activation of atoms which, in the vicinity of a boundary and in the presence of a biasing effect, causes atom migration preferentially in one direction across the boundary. A biasing effect results from a chemical potential difference $\Delta\mu$ across the boundary. For normal grain growth in homogeneous systems the driving force is the reduction in grain boundary surface area or, conversely, the reduction in grain boundary curvature. Such a biasing effect is represented by the Gibbs Thompson expression, $\Delta\mu = -4\gamma\Omega/L$, where γ is the surface energy, Ω is the atomic volume and L is the average grain diameter (or size). Using this as the driving force, η is derived as [11, 12],

$$\eta = \frac{k_0\gamma\Omega\rho k^2}{\pi\kappa_0 c_0 L\beta_{\mathrm{HGG}}^3}\frac{F_D^2}{\Delta H_{coh}^3} \tag{3}$$

where the activation energy Q for an atom to jump across the boundary within the thermal spike, has been approximated as $Q = -\beta_{\mathrm{HGG}}\Delta H_{coh}$ with ΔH_{coh} the cohesive energy and β_{HGG} a positive constant. The constants k_0, κ_0 and c_0 are the frequency factor, thermal conductivity and heat capacity of the target respectively.

The ion-induced grain boundary mobility M_{ion} may be found by combining eqns. (1), (2) and (3) and substituting $\partial\mu/\partial x = \Delta\mu/\delta$ to give,

$$M_{ion} = -\frac{k_0\delta^2 k^2\Phi}{4\pi\kappa_0 c_0\beta_{\mathrm{HGG}}^3}\frac{F_D^2}{\Delta H_{coh}^3} \tag{4}$$

It is observed through this expression that the thermal spike model relates ion-induced grain growth to both irradiation effects (F_D) and material properties (ΔH_{coh}).

3. Application of model to experimental results

The thermal spike model predicts a linear dependence of the ion-induced grain boundary mobility on the parameter $F_D^2/\Delta H_{coh}^3$. This dependence can be evaluated with respect to seven sets of experimental grain growth data on elemental and coevaporated alloy films [1–7]. The data from these seven experiments were given as measured grain size L, as a function of ion dose Φ, and the ion–target combinations analyzed are listed in Table 1.

One of the difficulties encountered in comparing results from these different experiments is the variation in grain size measurement techniques used. The variety of techniques employed is due largely to the difficulty in applying standard grain size measurement techniques (e.g. intercept methods) to irradiated thin film microstructures. Tests of linearity predicted by eqn. (4) must therefore be restricted to data from a specific experiment rather than attempting to interpret the data from all seven experiments collectively. An additional caveat is required by the presence of the ion dose rate Φ in eqn. (4). The experiments described in ref. 6 did not contain dose rate information. Therefore, in order to be consistent, it was necessary to use a dose rate normalized mobility quantity M_{ion}/Φ, instead of simply M_{ion}.

Evaluation of the model requires determining F_D and ΔH_{coh} values for the various ion–target combinations and also deriving values of M_{ion}/Φ from the experimental grain growth data. Values of F_D were obtained from TRIM v.5.5 [14] calculations in which 1000 histories

TABLE 1. Parameters of interest in thermal spike analysis of ion-induced grain growth experimental data

Film (at.%)	Energy (keV) Ion	Reference	ΔH_{coh}[a] (eV)	F_D (eV Å^{-1})	$L^n - L_0^n = K\Phi$ fit parameters			$F_D^2/\Delta H_{coh}^3$ (Å^{-2} eV^{-1})	M_{ion}/Φ ($\times 10^6$ Å^4 eV^{-1})	β_{HGG}
					K (Å^n cm^2)	L_0 (Å)	n			
Pt-15Ti	1700, Xe	1	6.21	425	1.00×10^{-9}	84	2.4	754	0.89	0.05
Pt-15V	1700, Xe	1	6.04	416	1.14×10^{-8}	68	2.8	785	1.57	
Ni-23Al	1700, Xe	1	4.43	355	1.41×10^{-8}	98	3.1	1450	0.45	
Pt-17Ni	1700, Xe	1	5.63	455	1.76×10^{-8}	105	2.8	1160	1.80	
Au-10Co	1700, Xe	1	3.83	400	8.59×10^{-6}	114	3.6	2847	5.24	
Au	200, Ar	2	3.81	91	8.72×10^{-9}	170	2.4	150	6.32	—
Pt	200, Ar	2	5.84	99	1.11×10^{-13}	141	1.0	49	0.02	
Ni	560, Xe	3	4.44	474	2.81×10^{-9}	87	2.7	2567	0.79	0.10
Ni	310, Kr	3	4.44	278	4.85×10^{-8}	91	3.3	883	0.66	
Ni	240, Ar	3	4.44	100	1.40×10^{-8}	88	3.3	114	0.32	
Pd	560, Xe	4	3.89	410	6.67×10^{-7}	84	3.4	2856	2.74	0.07
Pd	185, Ar	4	3.89	99	2.12×10^{-8}	92	3.0	167	0.95	
Pd	100, Ne	4	3.89	39	4.25×10^{-8}	90	3.2	26	0.84	
Cu	200, Ar	5	3.49	100	1.34×10^{-5}	148	4.1	235	1.33	—
Co	600, Xe	6	4.39	455	2.70×10^{-8}	121	3.2	2447	0.60	—
Ni	600, Xe	6	4.44	485	3.07×10^{-7}	110	2.6	2687	0.19	
V	600, Xe	6	5.31	324	6.33×10^{-7}	104	4.1	701	0.14	
Cr	600, Xe	6	4.10	382	1.89×10^{-9}	84	3.1	2117	0.27	
Ti	600, Xe	6	4.85	230	1.98×10^{-9}	92	3.2	464	0.08	
Au	200, Xe	7	3.81	389	3.09×10^{-9}	355	2.1	2736	96.20	—
Au	80, Kr	7	3.81	192	1.06×10^{-4}	342	3.3	667	10.90	

[a]Alloy cohesive energies determined from elemental values according to $\Delta H_{coh} = f_A \Delta H_{coh(A)} + f_B DH_{coh(B)} + \Delta H_{mix}$, where f_A and f_B are the atom fractions of the A and B alloy elements respectively, and ΔH_{mix} is the heat-of-mixing (see ref. 1).

were run under full cascade conditions with displacement energies set equal to 25 eV. The F_D values quoted in Table 1 represent the total ion and recoil energy deposited in nuclear interactions. Values for cohesive energy were taken from ref. 15.

Experimentally derived values of the normalized mobility M_{ion}/Φ were obtained using the following procedure. Grain size L *vs.* ion dose Φ data were fit according to the expression,

$$L^n - L_0^n = K\Phi \tag{5}$$

with L_0 the best-fit initial grain size, n the best fit growth exponent and K a best fit constant. This expression is analogous to that used to describe the kinetics of isothermal normal grain growth with time t replacing ion dose Φ. Curve fits were restricted to ion doses Φ such that $0 \leqslant \Phi \leqslant 3 \times 10^{15}$ cm^{-2} in order to avoid large dose regimes in which grain size saturation was observed to occur in certain samples. The resulting fit parameters for the experiments of interest are found in Table 1. Equation (5) was then differentiated with respect to Φ to obtain an expression for $dL/d\Phi$. Using the fit parameters, the normalized mobility was then found from the slope of $dL/d\Phi$ values *vs.* $\partial\mu/\partial x = -4\gamma\Omega/\delta L$ values (see eqn. (1)) evaluated over a range of ion dose. For this portion of the analysis doses were restricted such that $\Phi \geqslant 10^{14}$ cm^{-2} in order to avoid contributing data from very small grain sizes. The spike-induced grain growth process, as described above, is not likely to be a valid description for the very small grain size regime in which the dimensions of disorder induced by thermal spikes is greater than or equal to the size of the grains.

The results of this thermal spike analysis applied to the seven sets of experimental grain growth data are displayed in Fig. 1(a). Linear fits were determined for each group consisting of more than two data points. Also included in Fig. 1(b) is a comparison of the normalized mobility as a function of F_D for the same group of experiments.

4. Discussion

Examination of the thermal spike analysis results shown in Fig. 1(a) support the linearity predicted by eqn. (4). For each individual experiment studied, with the exception of one (ref. 6), the trend is present that larger values of $F_D^2/\Delta H_{coh}^3$ result in larger values of normalized mobility. The larger variation in the slopes of these lines is believed to be attributable to the variations in grain size measurement techniques as discussed above. Variations may also be due to other effects. In the nickel [3] and Ni–Al samples [1], it was reported that irradiation induced the formation of the hexagonal close-packed

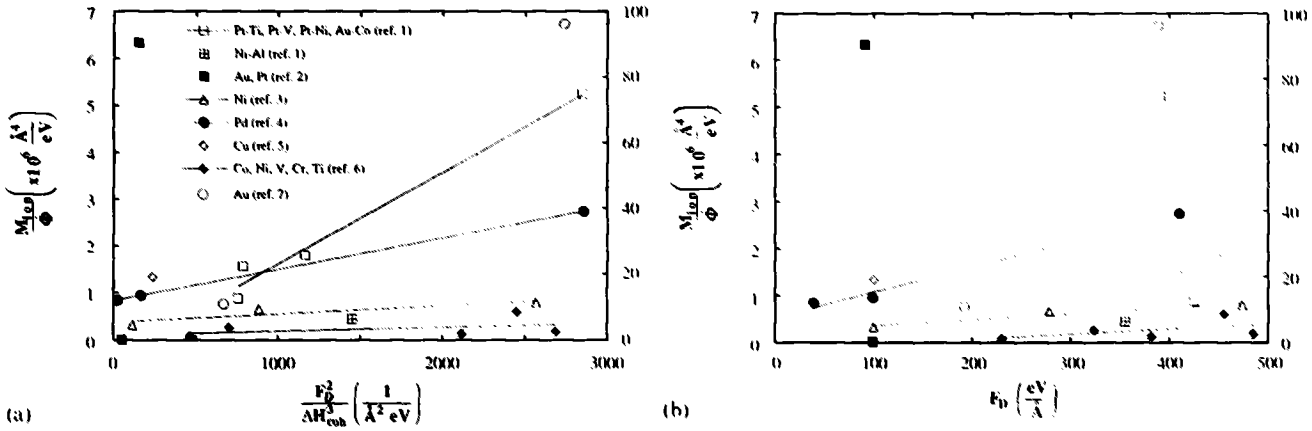

Fig. 1. (a) Thermal spike analysis of experimental ion-induced grain growth data showing the normalized mobility $M_{ion}\,\Phi$ as a function of the parameter $F_D^2/\Delta H_{coh}^3$. (b) Variation in normalized mobility with F_D for the same experiments as in (a). For both plots, the normalized mobility values for the gold data from ref. 7 are referenced with respect to the axis on the right.

(h.c.p.) phase in addition to the face-centered cubic (f.c.c.) phase. The presence of this phase may have lowered grain boundary mobility in these samples. For this reason the Ni–Al data point in Fig. 1(a) was excluded from the linear fit evaluated for the coevaporated film data.

The thermal spike analysis results from Fig. 1(a) may be contrasted with those in Fig. 1(b) in which normalized mobility is observed as a function of F_D alone. A purely collisional model of ion-induced grain growth (such as Atwater's [7]) would predict that the normalized mobility should increase linearly with increasing F_D (for the same displacement energies). As seen in Fig. 1(b) such a linear dependence exists for three sets of data, however it is notably absent in the data of Li *et al.* [2] (gold, platinum) and Alexander *et al.* [1] (coevaporated films). Films in both of these data sets were expected to behave collisionally the same (similar F_D and displacement energies) but clearly there are large variations in mobility among them. Again, the data from ref. 6 appear nearly insensitive to variations in F_D.

It is unclear why the data in ref. 6 are inconsistent with the trends observed in the thermal spike analysis of the other experiments. A possible concern may be the reactive nature, with respect to oxidation, of most of the films used in the study. The formation of oxide during film deposition or during irradiation might well be expected to decrease the mobility of grain boundaries or substantially alter cohesive energies. It is further noted that these elements span a variety of crystal structures, suggesting that the grain growth process may be correlated with structure.

Additional support for the thermal spike model of ion-induced grain growth is provided by comparison with ion beam mixing. A similar thermal spike approach has been successful in describing variations in ion beam mixing rates observed among a variety of bilayer metallic thin films [10]. As was done above, the ion beam mixing model scales the activation energy for atom migration with the average alloy cohesive energy, $Q = \beta_{IM}\Delta H_{coh}$, with β_{IM} the scaling constant for ion mixing (IM). Using the data in Fig. 1(a), it is possible to estimate the proportionality constant β_{IIGG} for ion-induced grain growth experiments, for comparison with β_{IM}. The slope m' determined from the plot of the normalized mobilities M_{ion}/Φ, *vs.* the parameter $F_D^2/\Delta H_{coh}^3$ shown in Fig. 1(a) can be used to find β_{IIGG} for the different groups of data. From eqn. (4), β_{IIGG} is expressed as,

$$\beta_{IIGG} = \left(\frac{k_0\delta^2 k^2}{4\pi\kappa_0 c_0 m'}\right)^{1/3} \tag{6}$$

Values for the constants in the parentheses may be estimated and are given in Table 2. Because of uncertainty of the environment within a thermal spike, average, generic values were chosen for the material constants: δ, Ω, k_0, γ, κ_0 and c_0. Using the values in Table 2, the proportionality constants are determined for the groups of data consisting of two or more data points. The values of β_{IIGG}, listed in Table 1, span a range $0.05 \leqslant \beta_{IIGG} \leqslant 0.10$. These values are less than the constant determined previously for ion beam mixing

TABLE 2. Values of constants used in ion-induced grain boundary mobility analysis; material constants represent average, generic values applicable to all the targets

Constant	Value
k_0 (s^{-1})	3×10^{13}
δ (Å)	3
γ (eV cm^{-2})	3×10^{14}
Ω (Å^3)	15
c_0 (eV K^{-1} cm^{-3})	1.3×10^{19}
κ_0 (eV cm^{-1} K^{-1} s^{-1})	6.3×10^{18}
k (eV K^{-1})	8.62×10^{-5}

(IM) experiments, $\beta_{IM} = 0.14$ [10]. The fact that β_{IIGG} is only a factor 1.4–3.0 different from β_{IM} is quite remarkable since the two parameters were obtained from experimental data examining different phenomena (mixing *vs.* grain growth). Furthermore, the smaller values of β_{IIGG} are consistent with the idea that atomic diffusion across grain boundaries is easier, having a lower activation energy, than diffusion within the lattice.

Clearly, the thermal spike model as presented here represents a highly idealized picture of how ion irradiation affects grain growth. However, it does permit an analytical treatment of the grain growth process. The model does not take into account the nature of the cascade structure [16] which may reasonably be expected to vary considerably among different ion–target combinations and in turn lead to varying grain growth behavior. Also, this and previous models [7, 8] have ignored the possible effects presented by the film morphology. The large amounts of surface area present in all the thin film samples studied represent potential sources and sinks for defects produced during irradiation and may indeed impact on the ion-induced grain growth process in thin films. In spite of these concerns, the thermal spike approach does provide a framework in which to incorporate material properties (*i.e.* ΔH_{coh}) aside from those associated strictly with collisional effects. As demonstrated above, it is thus possible to account for different grain growth behavior observed in collisionally similar systems.

5. Conclusions

Ion-induced grain growth can be described by a thermal spike model in which irradiation-induced, cylindrical thermal spikes thermally activate atom jumps resulting in boundary migration. For elemental and homogeneous alloy films, in which grain growth is driven by boundary curvature, the model predicts a linear dependence of the ion-induced boundary mobility with the quantity $F_D^2/\Delta H_{coh}^3$, where F_D is the ion and recoil energy deposited in nuclear interactions and ΔH_{coh} is the cohesive energy.

The model was evaluated with respect to seven sets of previously published experimental ion-induced grain growth data. The results of all but one experiment supported the thermal spike model results. Combining analytical results of the model with the experimental data it was possible to determine the value of the proportionally constant relating the cohesive energy to the activation energy for grain growth. Depending on the experiment, the value of the constant spanned the range $0.05 \leqslant \beta_{IIGG} \leqslant 0.10$, which is less than the value previously determined for the thermal spike treatment of ion beam mixing ($\beta_{IM} = 0.14$), and therefore consistent with the idea that atom migration across grain boundaries is easier than migration within the lattice. The consistency of results from the analysis of an entirely different phenomenon, adds further credence to the thermal spike treatment of ion-induced grain growth.

Additional experiments are necessary, specifically designed to examine a broad range of F_D and ΔH_{coh} values and cascade structure, in order to evaluate the model's validity.

Acknowledgments

This work was funded under DOE contract W-31-109-ENG-38 (D. Alexander) and NSF grants DMR8603174 and DMR8903138 (G. Was).

References

1 D. E. Alexander, G. S. Was and L. E. Rehn, *J. Appl. Phys.*, *70* (1991) 1252.
2 J. Li, J. C. Liu and J. W. Mayer, *Nucl. Instrum. Methods B*, *36* (1989) 306.
3 J. C. Liu and J. W. Mayer, *Nucl. Instrum. Methods B*, *19/20* (1987) 538.
4 J. C. Liu, M. Nastassi and J. W. Mayer, *J. Appl. Phys.*, *62* (1987) 423.
5 J. C. Liu, J. Li and J. W. Mayer, *J. Appl. Phys.*, *67* (1990) 2354.
6 P. Borgesen, D. A. Lilienfeld and H. Massad, in H. A. Atwater, F. A. Houle and D. H. Lowndes (eds.), *Surface Chemistry and Beam–Solid Interactions*, Materials Research Society, Pittsburgh, PA, 1991, p. 393.
7 H. A. Atwater, C. V. Thompson and H. I. Smith, *J. Appl. Phys.*, *64* (1988) 2337.
8 J. C. Liu, *Thesis*, Cornell University, Ithaca, NY, 1989.
9 L. E. Rehn and P. R. Okamoto, *Nucl. Instrum. Methods B*, *39* (1989) 104.
10 M. Van Rossum and Y-T. Cheng, in F. H. Wohlbier (ed.), *Ion Implantation 1988*, Trans Tech Publications Ltd., Switzerland, 1988, pp. 1–31.
11 D. E. Alexander and G. S. Was, in C. V. Thompson, J. Y. Taso and D. J. Srolovitz (eds.), *Evolution of Thin Film and Surface Microstructure*, Materials Research Society, Pittsburgh, PA, 1991, p. 205.
12 D. E. Alexander, *Thesis*, University of Michigan, Ann Arbor, MI, 1990.
13 G. H. Vineyard, *Radiat. Eff.*, *29* (1976) 245.
14 J. P. Biersack and L. G. Haggmark, *Nucl. Instrum. Methods*, *174* (1980) 257.
15 C. Kittel, *Introduction to Solid State Physics*, Wiley, New York, 1976, p. 74.
16 F. Rossi and M. Nastasi, *J. Appl. Phys.*, *69* (1991) 1310.